

Magnetic Short-range Order in Pt-Mn Spin-glass Alloys

Miwako TAKAHASHI, Masaomi HASHIMOTO, Ken-ichi OHSHIMA,
Yukio NODA,¹ Naohisa TAKESUE² and Toetsu SHISHIDO³

Institute of Materials Science, University of Tsukuba, Tsukuba, Ibaraki, 305-8573, Japan

¹*Research Institute for Scientific Measurements, Tohoku University, Sendai, 980-8577, Japan*

²*Neutron Scattering Laboratory, Institute for Solid State Physics,
University of Tokyo, Tokai, Ibaraki, 319-1106, Japan*

³*Institute for Materials Research, Tohoku University, Sendai, 980-8577, Japan*

The neutron diffraction measurements were carried out on the spin-glass alloys of Pt-12 and 16 at.% Mn with different atomic arrangements. Magnetic diffuse maximum is observed at $(1/2, 0, 0)$ in the samples of annealed and quenched 12 at.% Mn and quenched 16 at.% Mn. In the annealed sample of 12 at.% Mn, the shape is quite anisotropic with splitting. Besides the diffuse maximum, weak ferromagnetic scattering is observed in all the samples. The magnetic short-range order (MSRO) in the alloys is discussed in terms of a modulated structure of spin-density wave (SDW) and a ferromagnetic correlation, both of which are closely related to the atomic order.

KEYWORDS: magnetic short-range order, spin-density wave, Fermi surface nesting, atomic short-range order, spin-glass

§1. Introduction

Pt-Mn alloys with low Mn concentration have been regarded as the prototype systems exhibiting spin-glass behavior. In the previous study of the magnetic susceptibility measurement, the typical spin-glass behavior, i.e., the cusp anomaly at the freezing temperature T_g and remanent magnetization below T_g , was observed in a wide range of Mn concentration of 0.05 to 15 at.% Mn.¹⁾ The freezing temperature increases continuously with increasing Mn concentration. However, the paramagnetic Curie temperature θ changes drastically from -45 K in 10 at.% Mn to 100 K at 15 at.% Mn. The fact indicates that a ferromagnetic correlation begins to be dominant around the concentration owing to the ferromagnetic structure of the ordered Pt₃Mn.²⁾

The atomic structure of Pt rich Pt-Mn alloys has a fcc fundamental structure at high temperature and forms a Cu₃Au-type superlattice structure with cubic symmetry below order-disorder transition temperature T_c . In a disordered state, our x-ray and neutron scattering measurements revealed that the atomic short-range order (ASRO) has a tendency of the Cu₃Au-type order with the correlation between consecutive (111) planes of Pt or Mn atoms.³⁾

From the recent observation of magnetic satellite diffuse peaks in neutron scattering experiments, the spin-glass behavior in the alloys of Cu-Mn, Pd-M and Pt-M (M is 3d element) is explained by the model of SDW cluster in which short-ranged correlation of SDW fluctuates dynamically.⁴⁻⁸⁾ The origin of SDW is regarded to be the nesting of the flat Fermi surfaces in these alloys. The satellite peaks appear in reciprocal lattice at the positions given by a wave-vector \mathbf{Q} spanning the flat Fermi surfaces. In Cu-Mn alloys, \mathbf{Q} is nearly along [110] and 12-fold degeneracy in the direction of \mathbf{Q} results the

satellite peaks at $(1, 1/2 \pm \delta, 0)$ and at symmetry-related positions. On the other hand, the direction of \mathbf{Q} is nearly along [100] and the SDW peaks appear at $(1 \pm \delta, 0, 0)$ and at equivalent symmetry positions in Pd-M and Pt-M alloys. As for the Pt-Mn alloy, diffuse satellite peaks were observed at the positions with $\delta = 1/2$ in Pt-8.8 at.% Mn.³⁾

We performed neutron diffraction measurements on Pt-12 and 16 at.% Mn in order to study MSRO under different atomic arrangements. Magnetic structure of the two types of MSRO; a modulated correlation of SDW and a ferromagnetic one corresponding to the ferromagnetic Pt₃Mn, is discussed.

§2. Experimental

The samples we measured are single crystals grown by the Bridgman technique at Tohoku University. Each of them has a volume of about 1cc. They were annealed or quenched before the measurements for the different atomic arrangements in the samples. As the quenched samples, they were quenched into ice water after annealing at 850 °C for 12 at.% Mn and 1000 °C for 16 at.% Mn. The annealed samples were prepared by gradual cooling of them to room temperature (R.T.) after annealing at the temperature of 400 °C for 12 at.% Mn and 600 °C for 16 at.% Mn. The atomic order in the samples was investigated by x-ray and neutron scattering measurements at R.T.. In the samples of 12 at.% Mn, T_c is rather low (around 300 °C) and therefore, Cu₃Au-type atomic order is short-ranged (long-ranged) in the quenched (annealed) sample. In the samples of 16 at.% Mn, Cu₃Au-type atomic order is long-ranged in both the annealed and the quenched samples because of much higher T_c . On the other hand, the [111] layered correlation is always short-ranged in all the samples though its correlation length is much longer in the annealed samples than

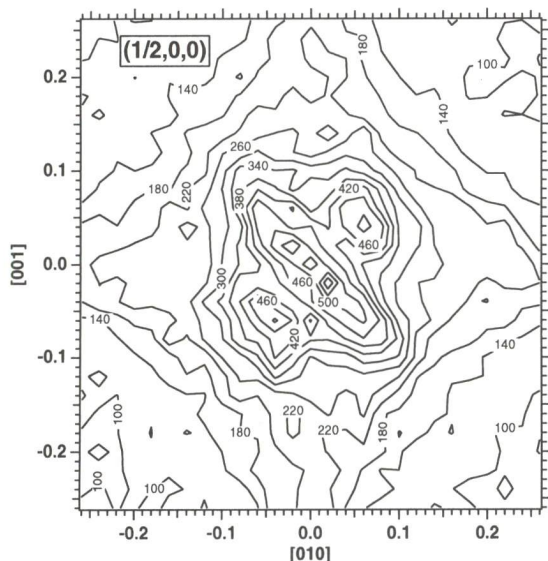


Fig.1. Scattering intensity contour map around $(1/2, 0, 0)$ on the (100) scattering plane taken at 7 K for the annealed 12 at.% sample.

in the quenched ones.

The freezing temperature T_g determined by the susceptibility measurements is 20 K for the annealed and 23 K for the quenched sample of 12 at.% Mn, and 28 K for both the annealed and the quenched samples of 16 at.% Mn.

Neutron scattering measurements were carried out using FOX spectrometer installed at the pulsed spallation-neutron source (KENS) in KEK, and FONDER spectrometer recently installed at T2-2 beam port of the thermal guide at the JRR-3M reactor in JAERI.⁹⁾ FOX is a single crystal diffractometer using the time-of-flight (TOF) Laue technique, while FONDER is a four-circle diffractometer with monochromatized neutrons.

§3. Results

In the measurements using FOX spectrometer, diffuse maximum is observed at around $(1/2, 0, 0)$ in the annealed and the quenched samples of 12 at.% Mn and with very low intensity, in the quenched sample of 16 at.% Mn. In the annealed sample of 16 at.% Mn, we could not detect the magnetic intensity at $(1/2, 0, 0)$ probably because a long tail of the strong intensity at (100) superlattice reflection smeared the weak intensity at $(1/2, 0, 0)$. The strong tail is caused by the anisotropic shape of the resolution of pulsed neutrons. In the annealed sample of 12 at.% Mn, the intensity distribution appears to be quite characteristic; it is a disklike-shape with its plane normal to the $[100]$ axis and in it, a splitting is superimposed. The same anisotropic diffuse maximum is also observed at $(3/2, 0, 0)$. For the detailed structure of the diffuse maximum, the measurement was performed with FONDER spectrometer. The observed diffuse pattern around $(1/2, 0, 0)$ in (100) scattering plane at 7 K is shown in Fig.1. The shape is quite anisotropic with splitting which seems to be fourfold. Unfortunately, the contamination of higher order (100) reflection obscures the precise structure of the splitting. The intensity distribution in the quenched sample of 12 at.% Mn is, on the

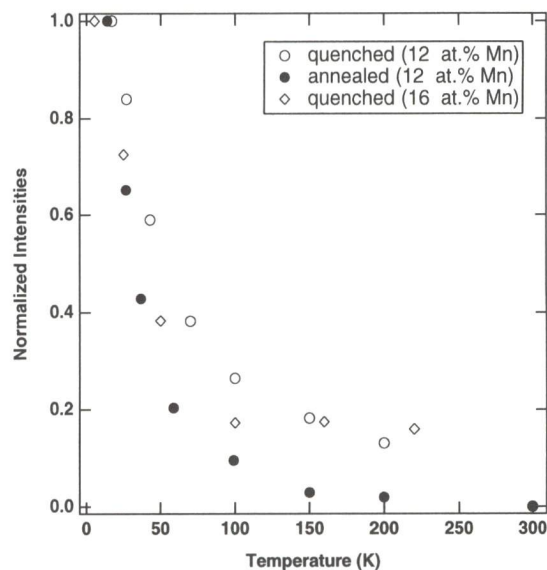


Fig.2. Temperature dependence of the normalized magnetic intensities integrated around $(1/2, 0, 0)$ diffuse maxima for the annealed and the quenched samples of Pt-12 at.% Mn and for the quenched sample of Pt-16 at.% Mn.

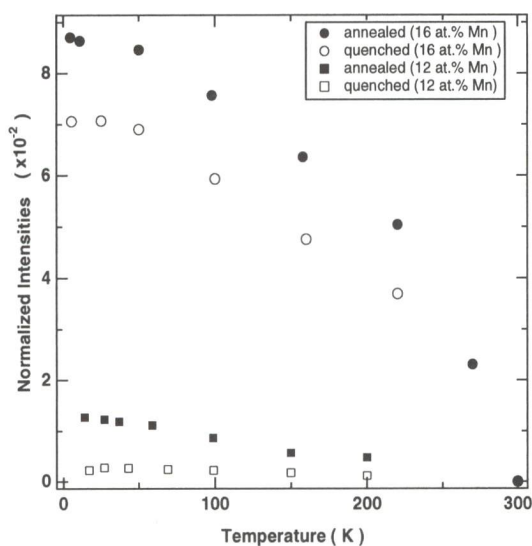


Fig.3. Temperature dependence of the normalized intensities integrated around (100) peak position for the annealed and the quenched samples of Pt-12 at.% and 16 at.% Mn.

other hand, almost isotropic with lower intensity. Since the intensity is much lower in the quenched 16 at.% Mn, its shape cannot be discussed with the present measurement. The temperature dependence of the normalized magnetic intensities integrated around $(1/2, 0, 0)$ is plotted in Fig.2. The intensities are subtracted by those at R.T. and are normalized with the values of the lowest temperature. They increase gradually with lowering the temperature from R.T. and then rapidly below around 50 K. No anomaly is observed at T_g . The behavior is common for the three samples indicating the same origin of the diffuse scattering.

In the intensity at (100) , magnetic scattering is observed together with the nuclear scattering due to the Cu_3Au -type atomic order. It increases with decreasing

temperature in all the samples. Fig.3 shows temperature dependence of the integrated intensities at around (100). The intensities are subtracted by those at R.T. and are normalized with the values of integrated (200) intensities at R.T.. The increase is remarkable in the samples of 16 at.% Mn. The convex curves in the figure are in sharp contrast to the concave curves in the Fig.2, showing that the two kinds of scattering are different in origin.

§4. Discussion

The features of the diffuse maximum at $(1/2, 0, 0)$ are quite similar to those in other Pt-M and Pd-M spin-glass alloys; the satellite diffuse intensity extends to higher temperature above T_g determined by the susceptibility measurement with no anomaly at T_g , and position of the maximum is on the [100] axis. The intensity persisting above T_g is ascribed to the inelastic component because of the coarse energy resolution in the measurements. The inelastic scattering is explained in terms of the dynamical fluctuation of the SDW clusters as suggested in other spin-glass alloys.⁵⁻⁸ The peak position of $(1/2, 0, 0)$ corresponds to $(1 \pm \delta, 0, 0)$ with $\delta = 1/2$, though diffuse maximum at $(3/2, 0, 0)$ is not observed in the quenched 12 and 16 at.% Mn. We believe that the intensity at $(3/2, 0, 0)$ is much weaker than that at $(1/2, 0, 0)$ owing to the abrupt reduction of Mn^{2+} scattering length so that the maximum is hidden by a strong tail of (200) fundamental reflection in the measurements with FOX spectrometer. The features thus indicate that the diffuse maximum at $(1/2, 0, 0)$ is due to the modulated correlation of SDW originated by the nesting effect of flat Fermi surface as in other Pt-M and Pd-M alloys. SDW diffuse maximum is also observed in 8.8 at.% Mn at the same position. The peak position is thus almost independent to the Mn concentration conflicting to other spin-glass alloys in which it varies continuously with the concentration of 3-d metal through the expansion of the Fermi surface.⁶⁻⁸ The fact implies that the Fermi level around the flat surface dose not change with the number of band electrons in Pt-Mn alloys.

The disklike-shaped diffuse maximum with splitting observed at $(1/2, 0, 0)$ in the annealed 12 at.% Mn is interpreted as follows. The SDW peaks appear at the surface of terminal points of \mathbf{Q} in the reciprocal lattice, and in Pt-Mn alloy with fcc fundamental structure, the positions are $(1 \pm \delta, 0, 0)$ and related-symmetry positions with $\delta = 1/2$. On the other hand, with the Cu_3Au -type long-range order, a new Brillouin zone smaller than that of fcc is formed. As the result, folding the new reciprocal lattice with the surface of \mathbf{Q} enhances the peaks at crossing around $(1/2, 0, 0)$. The idea is illustrated in Fig.4. It explains the characteristic diffuse maximum in the annealed 12 at.% Mn quantitatively. It is based on the Fermi surface imaging idea originally proposed by Moss to explain the splitting of the diffuse spots in Cu-Au alloys above T_c ,¹⁰ which also explains the SDW peaks in Cu-Mn alloys. Further study on the split diffuse maximum is proceeding now and will be reported.

Though the Cu_3Au -type atomic order is long-ranged in 16 at.% Mn, the $(1/2, 0, 0)$ diffuse maximum appears quite differently; only very weak intensity is detected at

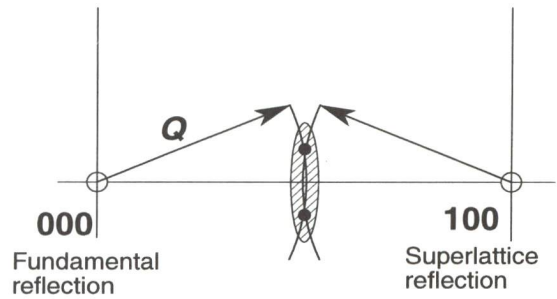


Fig.4. The diffuse scattering at $(1/2, 0, 0)$ in the annealed 12 at.% Mn. Solid lines; the surfaces of the vector \mathbf{Q} , closed circles; the enhanced peaks at crossing and shaded areas; magnetic diffuse scattering.

$(1/2, 0, 0)$ in the quenched sample. The fact is explained as that the ferromagnetic correlation begins to take over the SDW correlation in the alloys because the ordered Pt_3Mn is ferromagnetic. The ferromagnetic component is confirmed in the increasing intensities for lower temperature at (100) peaks. The remarkable increase in the 16 at.% Mn samples indicates higher development of the ferromagnetic short-range order in them. The result is consistent to the positive and increasing value of θ for Mn concentration higher than 10 at.%.¹

The present study shows that MSRO in Pt-Mn alloys is closely related to the atomic order and is dominated by both the modulated structure of SDW and ferromagnetic correlation of ordered Pt_3Mn ; former is more important for low Mn concentration and the later for more concentrated alloys. It is expected that the crossover from SDW to ferromagnet occurs between 12 to 16 at.%. Measurements on the samples around the Mn concentration is necessary to understand the relation between the two types of magnetic correlations and their contributions in the spin-glass behavior.

Acknowledgements

We would like to express our thanks to the staff of the sample preparation room of the Institute of Materials Research, Tohoku University for help in preparing single crystals. We are also grateful to Prof. M. Arai for his advice on neutron-scattering measurements at KENS. The present work is supported by Grand-in-Aid for Science Research (A, No.09354004) of Japan Society for Promotion of Science.

- 1) E. F. Wassermann: *Physica B&C* **109&110** (1982) 1936.
- 2) E. Krén, G. Kádár, L. Pál, J. Sólyom, P. Szabó and T. Tarnóczy: *Phys. Rev.* **171** (1968) 574.
- 3) M. Takahashi, S. Yoshimi, K. Ohshima and Y. Watanabe: *Phys. Rev. B* **61** (2000) 3528.
- 4) J. W. Cable, S. A. Werner, G. P. Felcher and N. Wakabayashi: *Phys. Rev. B* **29** (1984) 1268.
- 5) S. A. Werner: *Comments Cond. Mat. Phys.* **15** (1990) 55.
- 6) Y. Tsunoda, N. Himura, J. L. Robertson and J. W. Cable: *Phys. Rev. B* **56** (1997) 11051.
- 7) M. Hirano and Y. Tsunoda: *Phys. Rev. B* **59** (1999) 13835.
- 8) Y. Tsunoda: *J. Magn Magn. Matter* **177-181** (1998) 1337.
- 9) Y. Noda *et al.* (to be published).
- 10) S. C. Moss: *Phys. Rev. Lett.* **22** (1969) 1108.